

⁶ H. H. Wickman and G. K. Wertheim, *Phys. Rev.* **148**, 211 (1966).

⁷ C. E. Johnson, *Proc. Phys. Soc. (London)* **92**, 748 (1967).

⁸ H. J. Hrostowsky and A. B. Scott, *J. Chem. Phys.* **18**, 105 (1950).

⁹ J. H. Van Vleck, *The Theory of Electric and Magnetic Susceptibilities*, (Oxford U. P., London, 1932), p. 273.

¹⁰ It takes about 51 sec to generate a spectrum from the parameters D , E , g , H , A , and ΔE on the CMU Univac 1108 computer.

THE JOURNAL OF CHEMICAL PHYSICS VOLUME 57, NUMBER 10 15 NOVEMBER 1972

Electron Scattering by Molecules with and without Vibrational Excitation. VI. Elastic Scattering by CO at 6–80 eV*

DONALD G. TRUHLAR

Department of Chemistry,† University of Minnesota, Minneapolis, Minnesota 55455

AND

WALTER WILLIAMS AND SANDOR TRAJMAR

Jet Propulsion Laboratory,‡ Pasadena, California 91103

(Received 24 July 1972)

Elastic scattering differential cross sections in relative units for electron scattering from CO have been measured in the scattering angle range 15° – 85° and the impact energy range 10–80 eV. The experimental results are compared to the predictions of model polarized Born approximations using five different model interaction potentials. The model potential of Crawford and Dalgarno is in the best agreement with experiment, and agrees with experiment about as well as any local potential possibly can. Such a treatment is able to account for some of the features of the angle dependence of the differential cross sections. The largest discrepancies between theory and experiment are at 10 eV and at large scattering angles, and there are also smaller discrepancies at small scattering angles. Comparisons are also made to previous experimental studies by Ramsauer and Kollath and Arnot.

I. INTRODUCTION

This article reports the measurement of differential cross sections, DCS, in relative units for the fundamental process of elastic scattering of electrons by CO gas target in the intermediate energy range. Measurements were carried out for scattering angles θ in the range 15° – 85° for incident energies E of 10–80 eV utilizing a high-resolution electron spectrometer which resolved the elastic scattering from the vibrational excitation but not from the rotational excitation. The principal motivation for this work was (a) to provide accurate measurements of the angle dependence of the differential cross section over a wide angular range in the intermediate energy region for a molecular target with a permanent dipole moment and (b) to test quantum mechanical calculations of differential cross sections in the intermediate energy range.

The only modern measurements of the angle dependence of the differential cross sections for elastic scattering by molecules in the intermediate energy region have been for H_2 , N_2 , and O_2 ,^{1–4} and, at 20 eV only, for CO.⁴ Before 1936, there were more such studies,⁵ including two on CO—Ramsauer and Kollath's study⁶ in the energy range 0.99–6.25 eV for the angle range 15° – 167.5° , and Arnot's study⁷ at energies 30 and 83 eV for the angle range 10° – 120° . Elastic scattering differential cross sections for CO have also been obtained in the 205–500 eV region.^{7–9}

Although the plane wave approximation is not

completely valid at energies as low as those considered here, the polarized Born approximation with model interaction potentials has previously been somewhat successful for explaining the angle dependence of elastic scattering DCS at intermediate energies.^{1,4,10} We find this type of theoretical treatment also qualitatively explains the present results, with no new adjustable parameters.

In Sec. II, we describe the methods. In Sec. III, we present our experimental and theoretical results. In Sec. IV, we discuss the results.

II. METHODS

A. Experimental (Unnormalized)

The experiments were performed with a double electrostatic analyzer electron impact spectrometer. The spectrometer and the procedures for taking data have been described in detail previously.^{1,4,11}

Each impact energy was studied in three to five separate experiments (typically five). In each experiment, the elastic scattering intensity was measured at 15 angles in the range 15° – 85° . From all this data a best curve was drawn for the elastic intensity vs scattering angle in this angular range. Correcting this curve for the effective scattering path length at each angle and energy yields the differential cross sections as functions of scattering angle [$\text{DCS}(\theta, E)$ vs θ] in different arbitrary units at each energy. In general

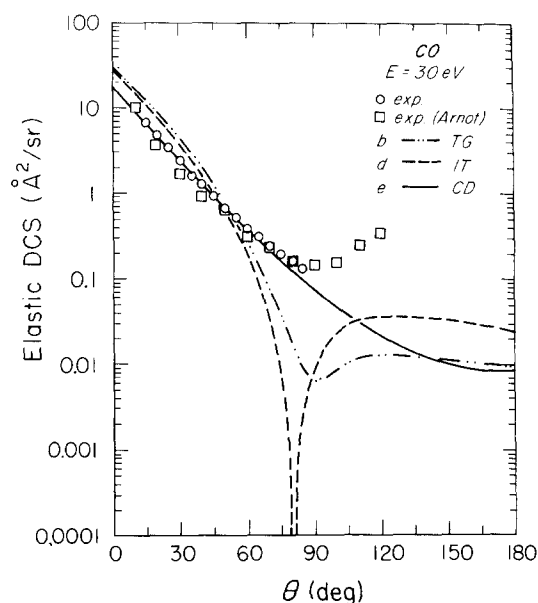


FIG. 1. Differential cross section as a function of scattering angle at 30 eV. The present experiments (circles) and Arnot's experiments (squares) are compared to three model polarized Born approximation calculations (curves as indicated). Both experiments are normalized to curve *e* at 50°.

we estimate the experimental errors are about 20%. At 10 and 15 eV impact energies we estimate the possible errors are 40%.

B. Theoretical

The quantum mechanical calculations are performed in the polarized Born approximation with five

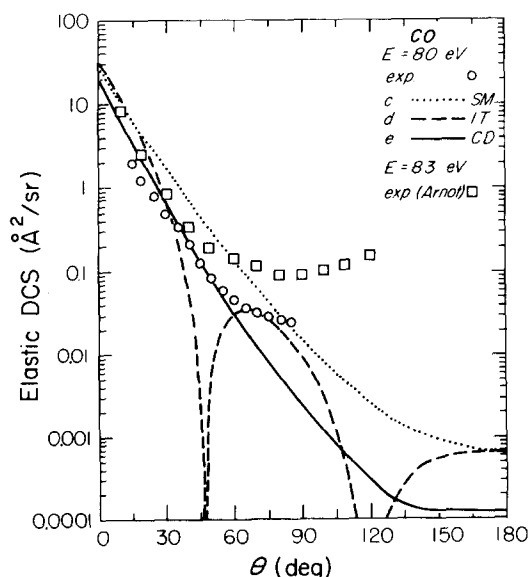


FIG. 2. Differential cross section as a function of scattering angle. The present experiments (circles) and three model polarized Born approximation calculations (curves as indicated) at 80 eV are compared to Arnot's experiments (squares) at 83 eV. The present experiments are normalized to curve *e* at 50°.

different approximate interaction potentials. These interaction potentials are in two cases direct copies of those used by previous workers (model *a*, Breig, and Lin¹²; model *e*, Crawford and Dalgarno¹³) and in three cases are based on models used by previous workers (model *b*, based on the work of Takayanagi and Geltman¹⁴; model *c*, based on the work of Sampson and Mjolsness¹⁵; and model *d*, based on the work of Itikawa and Takayanagi¹⁶). These potentials and the methods have been described in detail previously.⁴

Since none of the experimental results considered here resolve the rotational excitation from the elastic scattering, we will in all cases add the theoretical elastic scattering and rotational excitation, but call the sum elastic scattering.

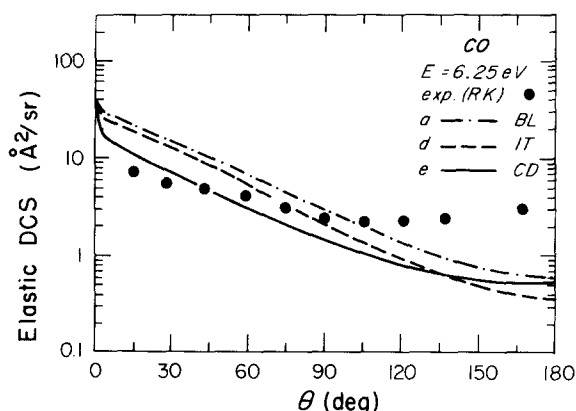


FIG. 3. Differential cross section as a function of scattering angle. The experiments of Ramsauer and Kollath (filled-in circles) are compared to three model polarized Born approximation calculations (curves as indicated). The experiment is normalized to curve *e* at 43°.

C. Experimental (Approximately Normalized)

We have previously found⁴ that model *e*, is in fairly good agreement with the elastic scattering DCS both for magnitude and for angle dependence at 20 eV in the 20°–85° scattering angle range. Hence, in order to place the present unnormalized experiments on an approximately absolute scale, we normalized our experimental DCS at each energy at the midpoint (50°) of the present experimental angular range to the calculated value in model *e*. From these curves we calculate partial elastic cross sections by

$$P_{2090}(E) = \int_{20^\circ}^{90^\circ} \text{DCS}(\theta, E) d\theta. \quad (1)$$

The approximately normalized $\text{DCS}(\theta, E)$ curves were extrapolated to 0° [using theoretical values of $\text{DCS}(\theta)/\text{DCS}(20^\circ)$ as a guide] and to 180° (using the old data of Bullard and Massey¹⁷ and Arnot⁷ and new measurements carried out in one of our laboratories on N₂ and CO up to 138° at 10 and 20 eV¹⁸ as guides). From these extrapolated curves we calculated approximate integral elastic cross sections Q at each energy

by

$$Q(E) = \int_0^{180} \text{DCS}(\theta, E) \sin\theta d\theta. \quad (2)$$

We estimate that the possible error in the small-angle extrapolation in $Q(E)$ is less than 10%, and the errors in the high-angle extrapolation causes errors in $Q(E)$ decreasing from less than 30% at 10 eV to less than 10% at 80 eV.

III. RESULTS

Figures 1 and 2 show the present experimental results for the DCS as functions of scattering angle at energies of 30 and 80 eV.

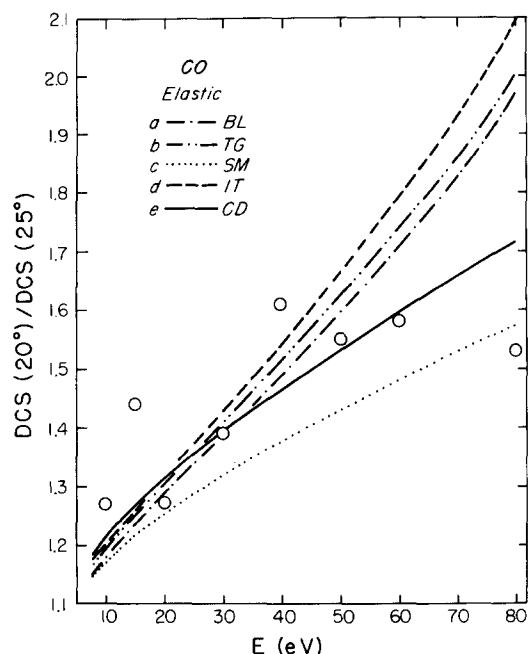


FIG. 4. Ratio of differential cross section at 20° scattering angle to differential cross section at 25° scattering angle as a function of impact energy. The present experiments (circles) are compared to five model polarized Born approximation calculations (curves as indicated).

These results are compared to the experimental results of Arnot.⁷ Arnot's data at both energies are in the same set of arbitrary units. For Figs. 1 and 2 we normalized all his data to the absolute scale by normalizing his 30 eV DCS at 50° to model *e*. This involves multiplying his data by 0.0238.

Figures 1–3 compare the present theoretical results for $\text{DCS}(\theta, E)$ to the experiments of Ramsauer and Kollath⁶ and Arnot and to some of the present experiments.

Figures 4 and 5 compare the present experiments with theory for $\text{DCS}(20^\circ)/\text{DCS}(25^\circ)$ and $\text{DCS}(30^\circ)$ as functions of E .

Figures 6 and 7 present all the present experimental DCS data as a function of momentum transfer q in

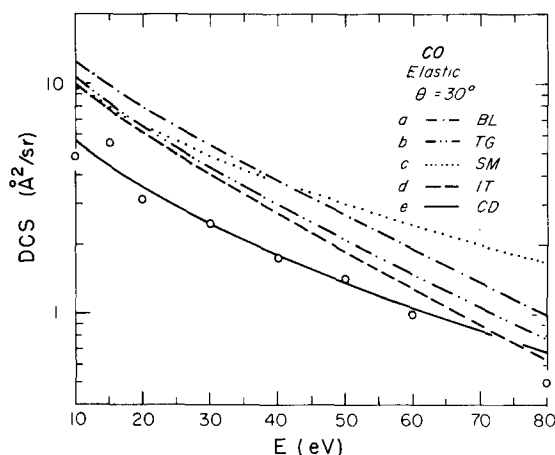


FIG. 5. Differential cross section at a scattering angle of 30° as a function of impact energy. The present experiments (circles) are compared to five model polarized Born approximation calculations (curves as indicated). The present experiments are normalized to curve *c* at a scattering angle of 50° at each energy.

atomic units where

$$q = 2k \sin \frac{1}{2}\theta, \quad (3)$$

and k in atomic units is the square root of E in rydbergs. In plane wave approximations with local potentials, such as the model polarized Born approximations used here, the DCS is a function of q alone, not q and E separately. Figures 6 and 7 also show, at small and large q , the DCS as a function of q as predicted by model *e*.

The theoretical and experimental values of the partial and integral cross sections are given in Tables I and II.

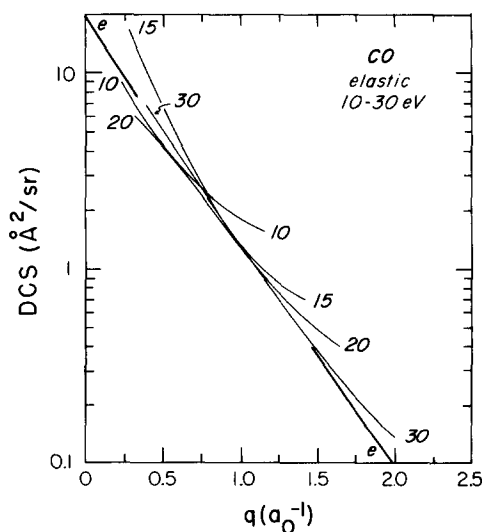


FIG. 6. Differential cross section as a function of momentum transfer. The present experiments at 10, 15, 20, and 30 eV impact energies (thin-line curves) are compared to model *e* polarized Born approximation calculations (curve marked *e*, which is shown only for small and large q).

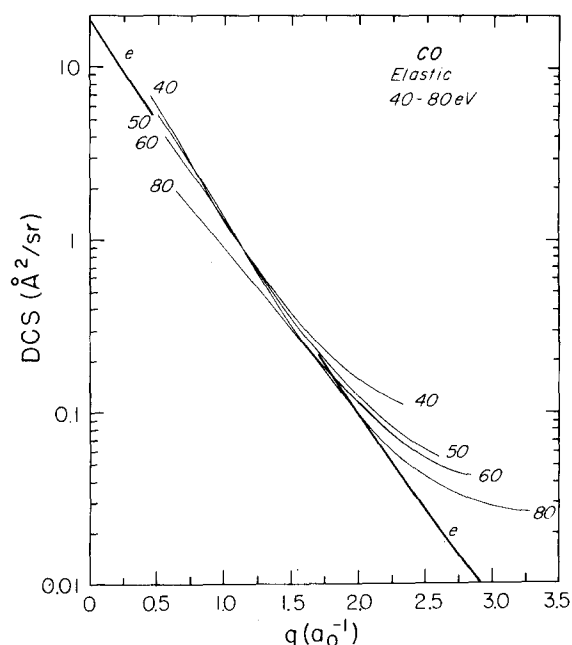


FIG. 7. Same as Fig. 6, except at 40, 50, 60, and 80 eV.

IV. DISCUSSION

Figures 1 and 2 show that the present experimental results are in good agreement with those of Arnot at 30 eV, but there is a discrepancy in angular dependence at 80–83 eV. The reason for the discrepancy is not known.

We believe our normalization of Arnot's and our own $\text{DCS}(\theta, E=30 \text{ eV})$ curves should be fairly accurate for the following reason. At 20 eV, we experimentally normalized our N_2 and CO elastic scattering cross sections.⁴ Our N_2 results agreed very well with those of Pavlovic *et al.*,³ providing a check on our procedure. Model *e*, with no new parameters, agreed with the magnitude and angle dependence of

TABLE I. Partial cross sections P_{2000} as a function of impact energy E .

| $E \text{ (eV)}$ | $P_{2000} \text{ (Å}^2\text{)}$ | | | | | |
|------------------|---------------------------------|----------|----------|----------|----------|----------|
| | Exptl ^a | <i>a</i> | <i>b</i> | <i>c</i> | <i>d</i> | <i>e</i> |
| 5 | | 54.2 | 45.5 | 44.8 | 43.0 | 24.9 |
| 10 | 15.4 | 30.8 | 25.4 | 28.1 | 23.6 | 14.6 |
| 15 | 11.9 | 19.9 | 16.3 | 20.1 | 14.9 | 9.9 |
| 20 | 7.2 | 13.8 | 11.4 | 15.2 | 10.2 | 7.2 |
| 30 | 4.6 | 7.8 | 6.4 | 9.8 | 5.6 | 4.4 |
| 40 | 3.2 | 5.0 | 4.0 | 6.9 | 3.6 | 3.0 |
| 50 | 2.3 | 3.5 | 2.8 | 5.2 | 2.4 | 2.2 |
| 60 | 1.64 | 2.6 | 2.0 | 4.0 | 1.75 | 1.62 |
| 80 | 0.82 | 1.51 | 1.1 | 2.6 | 0.98 | 1.00 |

^a Differential cross section normalized to model *e* at 50°.TABLE II. Integral cross sections Q as a function of impact energy E .

| $E \text{ (eV)}$ | Exptl | $Q \text{ (Å}^2\text{)}$ | | | | |
|------------------|-------|--------------------------|----------|----------|----------|----------|
| | | <i>a</i> | <i>b</i> | <i>c</i> | <i>d</i> | <i>e</i> |
| 5 | | 78.2 | 65.4 | 69.3 | 61.2 | 37.4 |
| 10 | 32 | 41.7 | 34.9 | 41.4 | 32.2 | 21.3 |
| 15 | 24 | 27.8 | 23.3 | 29.3 | 21.5 | 14.7 |
| 20 | 13.5 | 21.0 | 17.5 | 22.6 | 16.2 | 11.2 |
| 30 | 9.0 | 14.3 | 11.7 | 15.4 | 10.9 | 7.5 |
| 40 | 6.4 | 10.9 | 8.8 | 11.6 | 8.3 | 5.7 |
| 50 | 5.5 | 8.7 | 7.1 | 9.3 | 6.6 | 4.5 |
| 60 | 4.1 | 7.3 | 5.9 | 7.8 | 5.5 | 3.8 |
| 80 | 2.1 | 5.5 | 4.4 | 5.8 | 4.1 | 2.8 |

$\text{DCS}(\theta, E=20 \text{ eV})$.⁴ At 30 eV the experimental normalization is not known, but since model *e* agrees with the angle dependence of $\text{DCS}(\theta, E=30 \text{ eV})$ very well, and since 30 eV is so close to 20 eV, we expect model *e* agrees well with the (previously unknown) experimental magnitude. Thus we used model *e* to normalize the experimental results.

Once Arnot's data have been normalized at $E=30 \text{ eV}$, they are normalized at all E . A check on how well Arnot was able to measure the energy dependence of $\text{DCS}(\theta, E)$ can then be made by comparing his normalized $\text{DCS}(\theta, E=400 \text{ eV})$ curve to Bromberg's recent absolute measurement⁹ of this quantity. This comparison is given in Table III.

Comparison of the model polarized Born calculations with the present experiments shows that model *e* is in best agreement with experiment. The angular dependence of the cross section predicted by model *c* is in good agreement with model *e* and with experiment, but the magnitude predicted by model *c* is too large. The other three models do not predict the angular dependence as accurately. Some of these comparisons are shown in Figs. 1–3. Figure 3 shows that the model polarized Born calculations are much less accurate at 6.25 eV than at 20 eV (Ref. 4) or 30 eV (Fig. 1). Evidently the plane wave theory cannot be used at energies as low as 6.25 eV.

TABLE III. Comparison of Arnot's experimental $\text{DCS}(\theta, E=400 \text{ eV})$ in (angstroms)² per steradian (obtained by normalizing Arnot's arbitrary scale to model *e* at 30 eV and 50°) to Bromberg's experimental absolute $\text{DCS}(\theta, E=400 \text{ eV})$ in (angstroms)² per steradian.

| $\theta \text{ (deg)}$ | Arnot | Bromberg |
|------------------------|-------|-------------------|
| 19 | 0.92 | 6.15 |
| 29 | 0.37 | 0.90 ^a |
| 39 | 0.17 | 0.62 ^a |
| 49 | 0.083 | 0.30 ^a |

^a Linear interpolation.

Figure 4 compares the steepness of the experimental $\text{DCS}(\theta, E)$ curves for θ equals 20° and 25° to theory. Since the experimental data were averaged to obtain smooth curves (see Sec. II.A), this comparison is not sensitive to the exact choice of angles, e.g., a comparison (not shown) using θ equals 20° and 30° is very similar. This figure shows that model *e* is best agreement with experiment in general, but that model *c* may be better at high energy. The 80 eV point looks anomalous. Arnot's $\text{DCS}(\theta, 80 \text{ eV})$ curve is steeper and would agree better with theory. The theory does not predict the oscillations; however, these are within the 20% experimental error (see Sec. II.A) for the shape of the $\text{DCS}(\theta, E)$ functions, and they are probably just experimental scatter.

Figure 5 compares the experimental $\text{DCS}(30^\circ, E)$ curves to theory. Again models *c* and *e* predict the shape of the curve best, but model *c* gives too large a cross section. The comparison with model *e* shows the absolute experimental results at $E=30\text{--}60 \text{ eV}$ would hardly be changed if the experiment had been normalized at 30° instead of 50° . The absolute experimental data at $E=10\text{--}20 \text{ eV}$ would be changed by less than 20% if normalized at 30° instead of 50° . Again the possible errors seem largest at 80 eV, where a 40% change would be caused by normalizing at 30° instead of 50° . It is interesting to notice that the models *a*, *b*, and *d* predict a relatively large decrease in $\text{DCS}(30^\circ, E)$ in the $60\text{--}80 \text{ eV}$ interval, in good agreement with the present experiments. This may be fortuitous.

Figures 6 and 7 show that in the $15\text{--}60 \text{ eV}$ range there is at each energy a range of q where the experimental $\text{DCS}(q, E)$ appears to be a function of q alone and not E . Further, in this q range, the DCS is in good agreement with model *e*. But at large q , the $\text{DCS}(q, E)$ in every case ($E=10\text{--}80 \text{ eV}$) is larger than the predictions of the model polarized Born approximation. Further, the large- q data is a function of E as well as q , and thus no plane wave theory employing local potentials can explain the data. Model *e* is in good agreement with the $\text{DCS}(q, E)$ curves wherever these curves are independent of E and thus, it does as well as possible for a plane wave calculation employing a local potential. There is thus nothing to be gained as far as agreement over the whole energy range by readjusting the parameters of model potential *e*. Better agreement with experiment at large q will probably require considering distortion of the scattering electron wavefunction from a plane wave and exchange. Meaningful better agreement with experiment at small q may be possible merely by using an energy-dependent polarization potential and considering exchange; both polarization and exchange increase the forward cross section and both are more important at low energy.^{1,19} Distortion should be less important at small q . Since the plane wave theories are generally considered to be small- q approximations, it appears that the dis-

crepancies at small q will be harder to explain quantitatively. Even not considering the controversial 80 eV curve, the other curves differ at $q=0.5$ by an amount which is greater than the 20% estimated accuracy of the experimental angle dependence. More accurately normalized experiments are required to make a definitive test of theory at small q , but the results at this point suggest a nonlocal interaction is required. Especially the monotonic decrease of $\text{DCS}(q \cong 0.5, E)$ with increasing E for $E=40\text{--}80 \text{ eV}$ indicates that an energy-dependent polarization potential with less polarization at large E is called for.

The partial cross sections presented in Table I are presented because they are independent of extrapolation of the experimental data and thus provide a better test of theory than the integral cross sections. The energy dependence of the experimental $P_{2090}(E)$ curve agrees with model *e* better than any of the other models, but this is partly built in by the normalization procedure.

The experimental integral cross section for elastic scattering decreases rapidly in the $10\text{--}30 \text{ eV}$ energy range while the total cross section for all scattering processes²⁰ is fairly constant in this energy range. Arnot's results⁷ (normalized here), Bromberg's high energy results,⁹ and the present intermediate energy results are the only experimental results on the integral elastic cross section. Some of the experimental integral elastic cross sections in Table II are larger than the total cross sections.²⁰ Since this is impossible, it indicates that our normalization procedure has difficulties. Column *e* of Table II is probably more accurate than the experimental column, and it is probably the most accurate column in Table II. The only other result for integral elastic scattering with which Table II can be compared is the experimental result of Paper IV⁴ at 20 eV, which is 10 \AA^2 .

V. FINAL REMARKS

By treating electron-CO scattering as scattering of an electron off a rotator as we have done here and in Paper IV,⁴ we are replacing a 17-body problem (15 electrons and 2 nuclei) by a 3-body problem (1 electron and 2 electrostatically shielded nuclei). Thus we are reducing the many-body problem associated with the 15 electrons to a problem of one electron in a potential; we are replacing the nonlocal effects of exchange and dynamic polarization of the target by a local effective potential (or optical potential). The particular model potentials we use were developed for applications to low-energy integral scattering cross sections (model *a* contains a parameter which was selected¹² by comparison of plane wave calculations to vibrational excitation integral cross sections at $0.6\text{--}1.0 \text{ eV}$, models *b* and *c* contain parameters which were adjusted^{14,15} by comparison of distorted wave calculations to momentum transfer cross sections²¹ at about 0.6 eV and lower

TABLE IV. Integral cross sections (\AA^2) for total scattering (T), elastic scattering (E) and excitation of the $v'=1$ and $v'=2$ vibrational levels for H_2 , N_2 , and CO at the maximum in the cross section (which occurs at 3 eV or below) and at 20, 50, and 80 eV impact energies.

| Molecule | Process | Energy (eV) | | | |
|--------------|---------|--------------------|---------------------|----------------------|--------------------------|
| | | Max | 20 | 50 | 80 |
| H_2 | T | 16 ^a | 5 ^a | 4 ^a | |
| | E | | 4 ^b | 2 ^b | 1 ^b |
| | $v'=1$ | 0.5 ^c | 0.011 ^d | 0.010 ^d | 0.008 ^d |
| | $v'=2$ | 0.04 ^c | 0.0004 ^d | 0.0004 ^d | |
| CO | T | 34 ^a | 13 ^a | | |
| | E | | 10 ^e | 5 ^f | 2-3 ^f |
| | $v'=1$ | 1.5 ^g | 0.1 ^e | 0.01 ^h | |
| | $v'=2$ | 1.1 ^g | 0.02 ^e | | |
| N_2 | T | 26 ^a | 12 ^a | 10 ^a | |
| | E | | 10 ^e | 4 ^b | 2 ^h |
| | $v'=1$ | large ^g | 0.1 ^e | 0.002 ^{h,i} | 0.001-0.002 ^h |
| | $v'=2$ | | 0.02 ^e | | |

^a Reference 20.

^b Paper II (Ref. 1).

^c H. Ehrhardt, L. Langhans, F. Linder, and H. S. Taylor, Phys. Rev. **173**, 222 (1968).

^d Paper III [S. Trajmar, D. G. Truhlar, J. K. Rice, and A. Kuppermann, J. Chem. Phys. **52**, 4516 (1970)].

^e Paper IV (Ref. 4).

^f Paper VI (present).

^g A. V. Phelps, Rev. Mod. Phys. **40**, 399 (1968).

^h Estimated empirically using model polarized Born calculations as a guide.

ⁱ A. Skerbele, M. A. Dillon, and E. N. Lassettre, J. Chem. Phys. **49**, 3543 (1968).

energies, model d was used¹⁶ for close coupling calculations at 0.3-1.5 eV, and model e contains a parameter which was adjusted¹³ by comparison of close coupling calculations to momentum transfer cross sections²² at 0.03 eV). It is therefore very encouraging that these model potentials explain the angle-dependence of the intermediate-energy differential cross sections so well. Also, it is encouraging that model e , which is the most recent and the most accurately calibrated of the five potentials, works best. The model e potential has now been used successfully for

energies from 5×10^{-3} eV to 8.3×10^1 eV. Thus, except for energies where core-excited resonances are important,²³ we can apparently avoid treating the many-electron aspects of the problem for many purposes and we can use potentials calibrated at low energy to explain intermediate energy experiments.

APPENDIX

Table IV summarizes some of our results of Papers I-VI along with other relevant results in an attempt to give the over-all picture of the magnitudes of the integral cross sections.

* Parts of these results were reported at the 1969 Summer Meeting in the Far West of the American Physical Society, Honolulu, Hawaii, 3 September 1969.

† Work supported in part by the National Science Foundation under research grant No. GP 28684.

‡ Work supported in part by the National Aeronautics and Space Administration under Contract No. NAS7-100.

¹ S. Trajmar, D. G. Truhlar, and J. K. Rice, J. Chem. Phys. **52**, 4502 (1970), Paper II. See also erratum: *ibid.* **55**, 2004 (1971).

² S. Trajmar, D. C. Cartwright, and W. Williams, Phys. Rev. A **4**, 1482 (1971).

³ Z. Pavlovic, M. J. W. Boness, A. Herzenberg, and G. J. Schulz, Phys. Rev. A **6**, 676 (1972).

⁴ D. G. Truhlar, S. Trajmar, and W. Williams, J. Chem. Phys. **57**, 3250 (1972). Paper IV.

⁵ L. J. Kieffer, *Bibliography of Low Energy Electron Collision Cross Section Data* (Nat. Bur. of Stds., Washington, D.C., 1967), pp. 2, 3; At. Data **2**, 293 (1971).

⁶ C. Ramsauer and R. Kollath, Ann. Phys. **12**, 529 (1932).

⁷ F. L. Arnot, Proc. Roy. Soc. (London) **A133**, 615 (1931).

⁸ J. P. Bromberg, J. Chem. Phys. **50**, 3906 (1969).

⁹ J. P. Bromberg, J. Chem. Phys. **52**, 1243 (1970).

¹⁰ D. G. Truhlar, J. K. Rice, S. Trajmar, and D. C. Cartwright, Chem. Phys. Letters **9**, 299 (1971).

¹¹ S. Trajmar, D. C. Cartwright, J. K. Rice, R. T. Brinkmann, and A. Kuppermann, J. Chem. Phys. **49**, 5464 (1968).

¹² E. L. Breig and C. C. Lin, J. Chem. Phys. **43**, 3839 (1965).

¹³ O. H. Crawford and A. Dalgarno, J. Phys. B **4**, 494 (1971).

¹⁴ K. Takayanagi and S. Geltman, Phys. Rev. **138**, A1603 (1965). See also S. Geltman and K. Takayanagi, Phys. Rev. **143**, 25 (1966).

¹⁵ D. H. Sampson and M. C. Mjolsness, Phys. Rev. **140**, A1466 (1965).

¹⁶ Y. Itikawa and K. Takayanagi, J. Phys. Soc. Japan **27**, 1293 (1969).

¹⁷ E. C. Bullard and H. S. W. Massey, Proc. Roy. Soc. (London) **A133**, 637 (1931).

¹⁸ A. Chutjian and S. Trajmar (unpublished data).

¹⁹ D. G. Truhlar and J. K. Rice, J. Chem. Phys. **52**, 4502 (1970), Paper I. See also erratum: *ibid.* **55**, 2005 (1971).

²⁰ H. S. W. Massey, E. H. S. Burhop, and H. B. Gilbody, *Electronic and Ionic Impact Phenomena* (Clarendon, Oxford, England, 1969), 2nd. ed., Vol. II, p. 699.

²¹ A. G. Englehart, A. V. Phelps, and C. G. Risk, Phys. Rev. **135**, A1566 (1964).

²² R. D. Hake and A. V. Phelps, Phys. Rev. **158**, 70 (1967).

²³ L. Sanche and G. J. Schulz, Phys. Rev. A **6**, 69 (1972).